4th International Conference on Molten Slags and Fluxes, 1992, Sendai, ISIJ

DESILICONIZATION BY FLUX INJECTION AT THE BLAST FURNACE RUNNER

Takeshi Uchiyama, Kanji Takeda and Seiji Taguchi

Iron and Steel Research Labs., Kawasaki Steel Corp., Japan

Synopsis: Conditions to improve the reaction efficiency for desiliconization were studied by both a mathematical simulation and by flux injection experiments to a shallow metal bath installed in the blast furnace runner. The mathematical model took into account back mixing of the metal, the simultaneous decarburization reaction, acceleration of velocity of flux particles in an injection lance, and other operating conditions. The lance shape and carrier gas flow rate were particularly studied in the simulation, as these factors greatly affect the dispersion of flux particles into the molten metal. The simulation result shows that the horizontal section of the injection nozzle should be long and thin to accelerate the particles velocity and provide enough penetration. The oxygen utilization efficiency was increased by up to 60% by the applying results of the simulation.

Key words: blast furnace, casting shop, desiliconization, decarburization, pig iron pretreatment, mathematical simulation, lance conditions

1. Introduction

One problem of desiliconization in the blast furnace runner exists is the low reaction efficiency of the oxide flux due to insufficient reaction time. Slag formation in the torpedo car is a connected problem when the unreacted oxide flux is carried over into the torpedo. This problem can be solved by improving the reaction efficiency of desiliconization and removing the desiliconizing slag by a skimmer. Removing the desiliconizing slag is also effective for decreasing the consumption of dephosphorization flux in the next stage. The conditions required to improve the reaction efficiency were studied by both a mathematical simulation and by experiments for desiliconization by injecting flux into a shallow metal bath installed in the blast furnace runner.

2. Desiliconization by flux injection in the blast furnace runner

Fig. 1 shows schematically the desiliconization method by flux injection into a shallow metal bath which is installed in the runner of Chiba No.5 blast furnace. The dimensions of the hot metal bath are 4.0m long, 1.2m wide and 0.6m depth of hot metal. The desiliconization flux, which consists of fine iron ore and limestone in the ratio 9:1, is injected by immersion lance with carrier air. Hot metal and the desiliconizing slag is separated by a skimmer, and only the hot metal is run into a torpedo car. The desiliconizing slag is run out from the bath and falls into a slag pit.

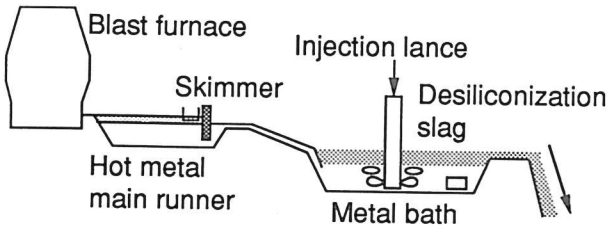

Fig.1 Schematic diagram of desiliconization method by injection at Chiba No.5 blast furnace.

3. Mathematical model for simulation

3.1 Flow pattern of metal in the bath and flux particle behavior

The circulating flow of metal in the desiliconization bath is schematically illustrated in Fig. 2. Two kinds of metal flow were considered, one being bulk flow caused by the inflow Q (m^3/s) of hot metal into the bath. The other is circulating flow q (m^3/s) induced by bubbles around the injection lance. Asai [1] was shown that the circulating flow could be represented by eq.1, assuming that the flow was controlled by the force of inertia. Therefore, eq.2 is obtained from eq.1.

$$v \propto (D\dot{\varepsilon}/\rho)^{1/3} \tag{1}$$

$$1/\tau \propto v/D = q/V \propto D^{-2/3}\dot{\varepsilon}^{1/3}\rho^{-1/3} \tag{2}$$

Where V is the volume of the hot metal bath (m^3)

D is the width of the bath (m)

ρ is the density of the metal (kg/m^3)

$\dot{\varepsilon}$ is the stirring energy (W/m^3)

v is the circulation velocity (m/s)

and τ is the time required for one circulation (s)

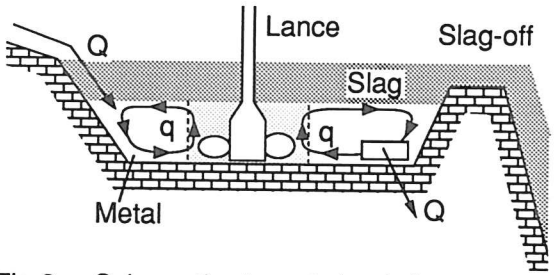

Fig.2 Schematic view of circulation flow in desiliconization bath.

It is very difficult to directly evaluate the circulating flow in the desiliconization bath. Therefore, experiments with water models of 1/10 and 1/3 scale were carried out in order to evaluate the circulation flow rate, the apparatus used being shown in Fig. 3. In this experiment, the impulse response was measured, and the result analyzed by the three-stage cascade model with a backmixing path between the stages. Fig. 4 shows the relationship between q/V and $D^{-2/3}\dot{\varepsilon}^{1/3}\rho^{-1/3}$, and from this figure, eq.3 was obtained.

$$q/V = 0.0642\, D^{-2/3}\dot{\varepsilon}^{1/3}\rho^{-1/3} \tag{3}$$

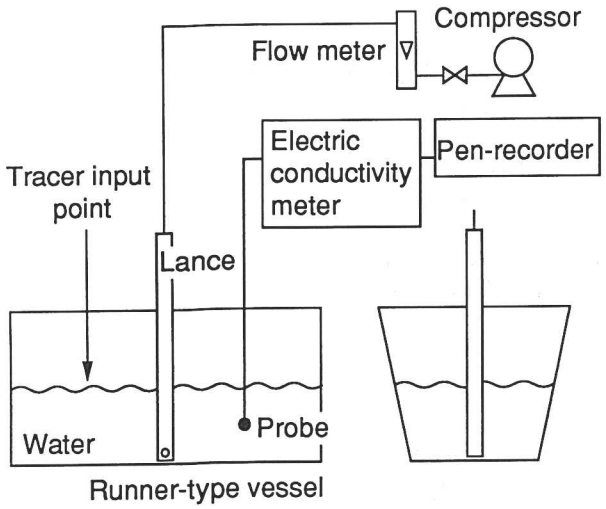

Fig.3 Experimental apparatus.

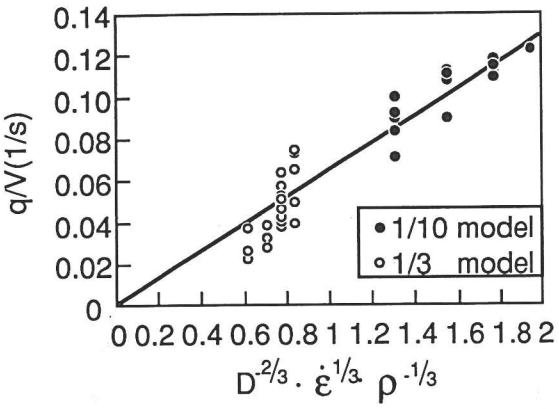

Fig.4 Relation between q/V and $D^{-2/3} \cdot \dot{\varepsilon}^{1/3} \rho^{-1/3}$.

The circulation flow rate, q, calculated by eq.3 is about 10 times greater than the inflow rate, Q, based on the hot metal production of a blast furnace. It is, therefore, clear that circulation flow characterize the flow pattern and mixing phenomena in the bath. Fig. 5 shows the experimental results for the impulse response of a Cu tracer in the metal bath, and the calculated result by the cascade model with backmixing, using q obtained from eq.3. Both are in good agreement, and it is thus apparent that the bath has nearly complete mixing. Thus, in the desiliconization model, the characteristics of the bath are regarded as complete mixing, with the flux particles rising in the molten metal at the same velocity as that of the circulation flow.

The desiliconization flux particles must penetrate into the hot metal through the bubble/metal interface and disperse into metal to react efficiently as illustrated in Fig. 6. In this model, the velocity of particles at the the nozzle tip was calculated by assuming that all particles have the same diameter represented by mean diameter (50% cumulative by mass) considering the acceleration by the carrier gas in the horizontal nozzle. The critical diameter for penetration was determined [2] on the basis of this calculated velocity.

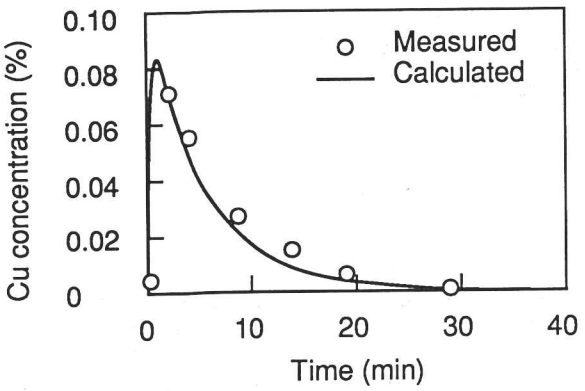

Fig.5 Impulse response of Cu tracer obtained in the metal bath at the blast furnace runner and that of calculation.

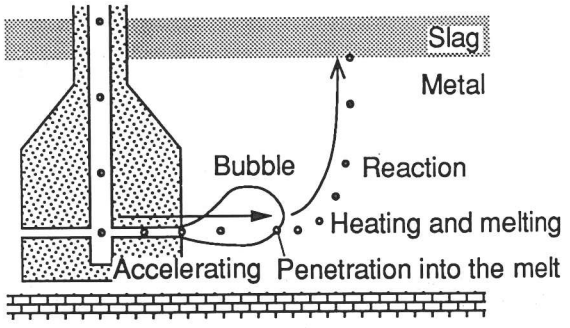

Fig.6 Behavior of flux particles around injection lance.

The particles which penetrate into the molten metal are heated, melted and reacted while rising with the circulation flow. It was assumed that the reaction time is the same as the rising time after melting. Any particles which could not penetrate into the hot metal would be remain within the bubbles and rises to the hot metal surface. These have very little reaction area compared with the particles which have penetrated into the metal. Therefore, the reaction amount by these particles is considered to be very small and has been neglected in this model.

3.2 Simultaneous desiliconization and decarburization reactions

Fig. 7 shows an example of the oxygen balance obtained from the flux, metal and slag composition. Most of the oxygen, which was provided with the flux and the carrier gas, was consumed in the desiliconization and decarburization reactions, the rest of the oxygen being removed with the slag. Therefore, in this model, simultaneous desiliconization and decarburization reactions have been assumed.

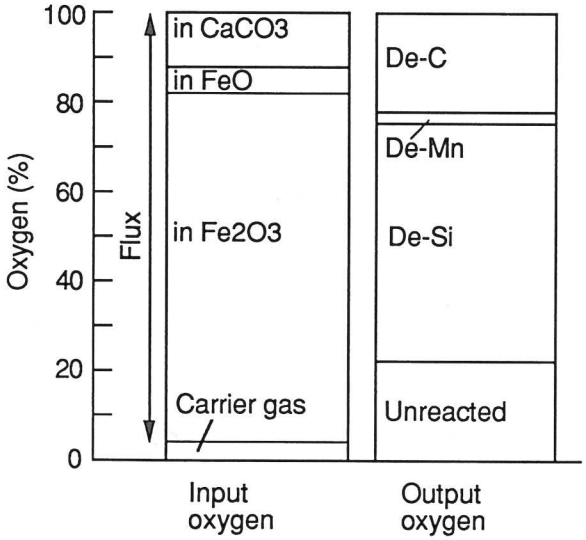

Fig.7 Example of oxygen balance of desiliconization by flux injecton.

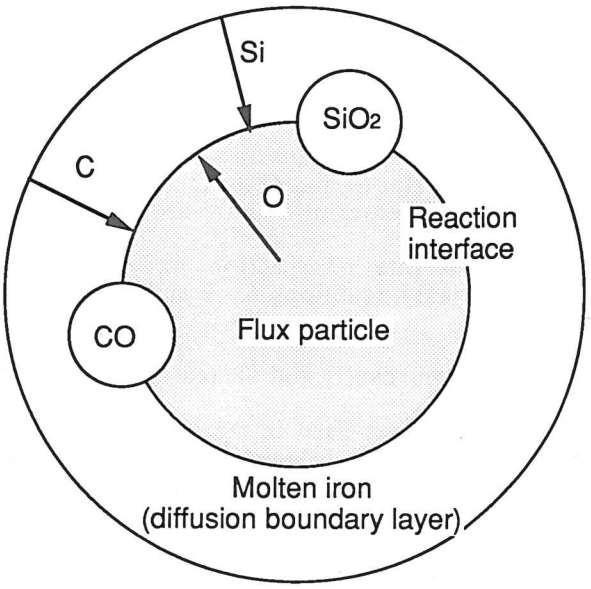

Fig.8 Schematical diagram of the desiliconization and decarburization reaction mechanism around flux particle.

According to Pan et al.[3], the reaction interface is the surface of the flux particles, the rate-determining step for the desiliconization reaction is the mass transfer of Si in the hot metal, the rate of the decarburization reaction is proportional to the oxygen content at the reaction interface, and the rate of supply of oxygen is controlled by the diffusion of (O) in the molten flux. A schematic diagram of the desiliconization and decarburization reaction mechanism around a flux particle is illustrated in Fig. 8. The desiliconization and decarburization reactions can be represented by the following equations:

$$\underline{Si} + 2(O) = (SiO_2) \quad (4)$$

$$\underline{C} + (O) = CO(g) \quad (5)$$

The rates of reaction are represented as follows:

$$R_{Si} = k_{Si} (C_{Si}^{b} - C_{Si}^{*}) A_i \quad (6)$$

$$R_C = k_C C_C^{*} A_i \quad (7)$$

$$R_O = k_O (C_O^{sb} - C_O^{s*}) A_i \quad (8)$$

Where R_{Si} is the rate of the desiliconization reaction (kg/s)
R_C is the rate of the decarburization reaction (kg/s)
R_O is the rate of mass transfer of (O) (kg/s)
k_{Si} is the mass transfer coefficient of Si (kg/m^{2}s) (= Nu ρ_l D_{Si}^* / d_p)
k_C is the rate coefficient of decarburization (kg/m^{2}s)
k_O is the mass transfer coefficient of (O) (kg/m^{2}s) (= Nu ρ_l D_O^s / d_p)
A is the area of the reaction interface (m^2)
C is the concentration (kg/kg)
D is the diffusion coefficient (m^2/s)
and d_p is the diameter of each particle (m)

The mass balance of oxygen at the reaction interface can be represented by eq.9.

$$R_O = R_{Si}\ 32/28 + R_C\ 16/12 \qquad (9)$$

Subscript Si and O mean silicon and oxygen, respectively, superscript s means the slag phase, and superscript b and * are the bulk and reaction interfaces, respectively.

Each rate of reaction under steady state conditions can be obtained by solving simultaneously equations 6 - 9 and the equilibrium of reactions 4 and 5.

4. Simulation results and measures to improve the efficiency of the desiliconization reaction

The values used in the calculation are shown in Table 1. The mass transfer coefficient of Si, k_{Si}, is about 1.1kg/m^{2}s for being no flow of hot metal. However, k_{Si} obtained from the experiment is 150kg/m^{2}s, this value being nearly 140 times larger value than the calculated value. The reason for this discrepancy is considered to have been due to an increase in the rate of mass transfer caused by the generation of CO gas. Mass transfer coefficient k_C obtained from the experiment is 0.01kg/m^{2}s. Fig. 9 shows a comparison of the oxygen utilization efficiency for desiliconization(η_{Si}) and decarburization(η_C) between the observed and calculated values. It is clear that the model can well simulate the dependence of η_{Si} and η_C on the initial concentration of Si($[Si]_i$).

Table 1 Base conditions used in calculation.

Mean diameter of flux	(μm)	200
Number of lance nozzle	(m)	2
Nozzle diameter	(m)	0.0216
Gas flow rate	(Nm^3 /s)	0.0433
Injection rate of flux	(kg/s)	1.0
Inflow rate of molten metal	(kg/s)	58.3
$[Si]_i$	(%)	0.5
Hot metal temperature	(K)	1773
Injection depth	(m)	0.45

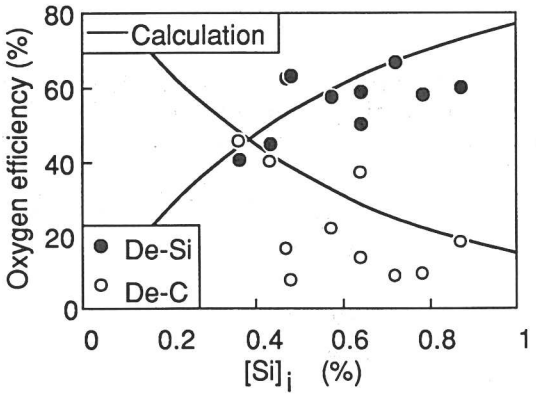

Fig.9 Comparison of observed oxygen efficiency and calculated one.

The velocity of particles at the nozzle tip needs to be high enough to penetrate into the hot metal through the bubble interface. The velocity of particles at the nozzle tip can be determined from the nozzle diameter and length (acceleration distance, L) for a constant carrier gas volume. Fig. 10 shows the effect of nozzle diameter on η_{Si}. η_{Si} improves as the nozzle diameter is reduced, but this effect becomes saturated at 15 - 20 mm in nozzle diameter under the conditions used. The reason for this is that the velocity of particles at the nozzle tip becomes so large that almost all of the particles penetrate into the metal. Fig. 11 shows the effect of acceleration distance on η_{Si}. η_{Si} improves as the acceleration distance is extended, but this effect also becomes saturated at L = 80 - 100 mm under the base conditions used. The simulation results are in good agreement with the experimental ones. η_{Si} was increased by up to 60% by the modifying the nozzle diameter and acceleration distance according to these results. Thus, the lance shape and injection conditions, which determine the velocity of particles at the nozzle tip, are very important for desiliconization by flux injection to the blast furnace runner.

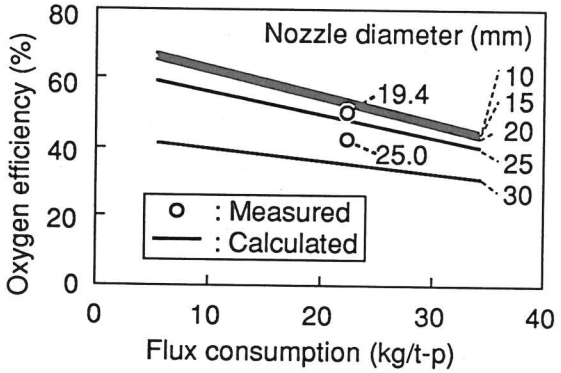

Fig.10 Effect of nozzle diameter on oxygen efficiency for desiliconization.

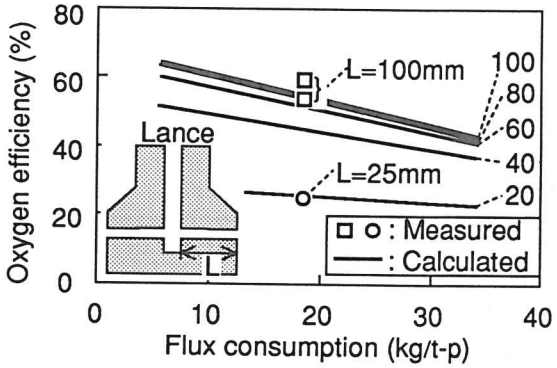

Fig.11 Effect of accelerating distance, L, on oxygen efficiency for desiliconization.

5. Conclusions

The conditions needed to improve the desiliconization reaction efficiency were studied by both a mathematical simulation and by experiments for flux injection to a shallow metal bath installed in the blast furnace runner. The effect of the initial silicon concentration in the metal was evaluated by considering a simultaneous decarburization reaction. A suitable lance shape to provide good penetration into the hot metal was found effective for improving the oxygen utilization efficiency for desiliconization.

References

1) S. Asai: 110th-101th Nishiyama Memorial Seminar, ISIJ, Kobe and Tokyo, 1984, 68.
2) K. Narita, T. Makino, H. Matumoto, and K. Ogawa: Tetsu to Hagane, 69 (1983), 392.
3) W. Pan, M. Sano, M. Hirasawa, and K. Mori: Tetsu to Hagane, 74 (1983), 61.